PROCEEDINGS OF SCIENCE

Differential jet cross sections at the CMS experiment

Anterpreet Kaur on behalf of CMS Collaboration*
Panjab University, Chandigarh
E-mail: anterpreet.kaur@cern.ch

We present measurements of differential jet cross sections over a wide range in transverse momenta from inclusive jets to multi-jet final states. Studies on the impact that these measurements have on the determination of the strong coupling α_S as well as on parton density functions are reported.

XXVI International Workshop on Deep-Inelastic Scattering and Related Subjects (DIS2018)
16-20 April 2018
Kobe, Japan

*Speaker.

PoS(DIS2018)091

1. Introduction

Jets are the experimental signatures observed in the detector in the form of narrow collimated cones of stable particles (mainly hadrons) produced by the hadronization of partons (quarks or gluons) in high-energy particle interactions. The theory of Quantum Chromodynamics (QCD) describes the strong interactions between the partons. In a hard scattering process, the partons produced with high-transverse momentum (p_T) give rise to a parton shower (PS) by emission of additional gluons and production of quark-antiquark pairs. This phase can be described by perturbative QCD (pQCD) approximations. In the non-perturbative (NP) regime, the colored partons hadronize into colorless hadrons in the form of collimated sprays called jets. Jets carry the significant information of the energy and direction of the initial partons and hence are important to study. The measurement of inclusive jet production ($p + p \rightarrow \text{jet} + X$) is vital to test predictions of pQCD as it probes the parton-parton interaction and is sensitive to the value of the strong coupling constant, α_S . It also provides the important constraints on the description of the proton structure, expressed by the parton distribution functions (PDFs).

CMS [1], one of the two general purpose detectors at the Large Hadron Collider (LHC) at CERN, is designed to see a wide range of particles and phenomena produced in high-energy proton-proton (pp) collisions in the LHC. This paper presents several studies of jet production performed by CMS with the data from proton-proton collisions taken at centre-of-mass energies ($\sqrt{s}$) of 8 and 13 TeV during Run 1 and 2 of the LHC respectively, from 2012 until 2016. The CMS detector covers a solid angle of almost 4π and consists of precise tracking devices around the interaction point, surrounded by calorimeters and muon chambers. The particles are reconstructed and identified using a particle-flow (PF) algorithm by combining the information from the individual sub-detectors [2]. The four-vectors of particle candidates, reconstructed by the above technique, serve as input to the anti-k_t jet clustering algorithm [3] and the clustering is performed within the FastJet package [4] using four-momentum summation. A factorized jet calibration procedure with corrections for pile-up and jet energy scale are applied. The data is also corrected for detector effects using an unfolding procedure which allows direct comparisons with next-to-leading order (NLO) theory as well as Monte Carlo (MC) predictions.

2. Inclusive jet production

The measurement of double-differential inclusive jet cross sections [5] has been performed as a function of jet p_T and absolute rapidity $|y|$ using the CMS data collected at $\sqrt{s} = 8$ TeV corresponding to an integrated luminosity of 19.7 fb^{-1}. This study covers a large range in jet p_T from 74 GeV up to 2.5 TeV, in six rapidity bins up to $|y| = 3.0$. To consider the region of low jet p_T, in particular from 21 to 74 GeV, a dedicated low-pileup 5.6 pb^{-1} data sample has been studied up to $|y| = 4.7$. The pQCD is supplemented by a small NP and electroweak (EWK) corrections and describes the data over a wide range of jet p_T and y as presented in Fig. 1 (left). This measurement also probes hadronic parton-parton interaction over a wide range of x and Q. The QCD analysis of inclusive jet measurements at 8 TeV together with HERA DIS measurements illustrates the potential of the high-p_T jet cross sections to provide important constraints on the gluon PDF in a new kinematic regime as shown in Fig. 1 (right). The high-p_T jet cross section measurements are

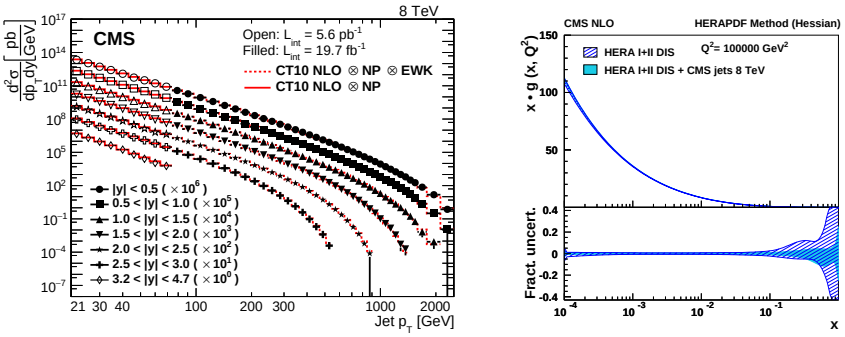

Figure 1: [5] Left : Double-differential inclusive jet cross sections as function of jet p_T for different $|y|$ bins at an interval of $\Delta\,|y| = 0.5$ are presented. Data (open points representing the low-p_T region, filled points representing the high-p_T one) and NLO predictions based on the CT10 PDF set corrected for the NP factor for the low-p_T data (solid line) and the NP and EWK correction factors for the high-p_T data (dashed line) are compared. Right : Gluon distribution as a function of x at the starting scale $Q^2 = 10^5$ GeV^2. The fit results to the HERA data and inclusive jet measurements at 8 TeV (shaded band), and to HERA data only (hatched band) [6] are compared with their total uncertainties determined by using the HERAPDF method. The bottom panel shows the fractional uncertainties.

used to extract the value of α_S. Using the probed p_T range and six different rapidity bins, the best fitted value of α_S at the Z boson mass scale is $\alpha_s(M_Z) = 0.1164^{+0.0060}_{-0.0043}$ using the CT10 NLO PDF set. The running of α_S as a function of the energy scale Q, is studied for nine different values of Q between 86 GeV and 1.5 TeV and is in good agreement with previous experiments as presented in Fig. 4.

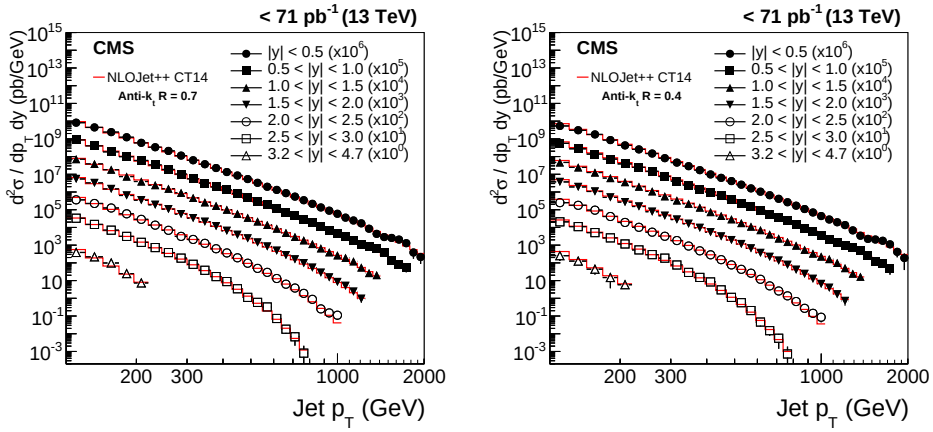

Figure 2: [7] : Double-differential inclusive jet cross sections as function of jet p_T for different $|y|$ bins at an interval of $\Delta\,|y| = 0.5$ for two jet sizes $R = 0.7$ (left) and $R = 0.4$ (right). Data (points) and predictions from NLOJET++ based on the CT14 PDF set corrected for the NP and EWK effects (line) are compared.

Similarly, a measurement of the double-differential cross sections as a function of jet p_T and absolute rapidity $|y|$ has been performed for two jet sizes $R = 0.4$ and 0.7 using data collected at $\sqrt{s} = 13$ TeV [7]. Data samples corresponding to integrated luminosities of 71 pb^{-1} and 44 pb^{-1} are used for absolute rapidities $|y| < 3$ and for the forward region $3.2 < |y| < 4.7$, respectively. The data and predictions at NLO in pQCD including corrections for NP and EWK effects are

compared in Fig. 2 for jet size $R = 0.7$ (left) and $R = 0.4$ (right). It is observed that jet cross sections for the larger jet size of $R = 0.7$ are accurately described, while for $R = 0.4$ theory overestimates the cross section by 5-10% almost globally. This measurement is a first indication that jet physics is as well understood at $\sqrt{s} = 13$ TeV as at smaller centre-of-mass energies in the phase space accessible with the new data.

3. Triple differential dijets

Measurements of dijet cross sections can be used to test predictions of pQCD at high energies as well as to constrain parton distribution functions (PDFs). Using CMS data collected at $\sqrt{s} = 8$ TeV, the triple-differential dijet cross sections have been measured as a function of the average transverse momentum $p_{T,avg} = \frac{1}{2}(p_{T,1} + p_{T,2})$ of the two leading jets, half of their rapidity separation $y^\star = \frac{1}{2}|y_1 - y_2|$ and the boost of the dijet system $y_b = \frac{1}{2}|y_1 + y_2|$ [8]. Data are found to be well described by NLO predictions corrected for NP and electroweak (EW) effects, except for highly boosted event topologies that suffer from large uncertainties in parton distribution functions (PDFs) as shown in Fig. 3 (left). For large values of y_b, the momentum fractions carried by the incoming partons must correspond to one large and one small value giving rise to same-side events, while for small y_b the momentum fractions must be approximately equal giving opposite-side events. In addition, for high jet p_T, x values are probed above 0.1, where the proton PDFs are less precisely known. It is observed in Fig.3 (right) that the precise data constrain the PDFs, especially in the highly boosted regime which probes the highest fractions x of the proton momentum carried by a parton. Also in a simultaneous fit, the value of $\alpha_s(M_Z)$ is extracted together with the PDFs giving $\alpha_s(M_Z) = 0.1199 \pm 0.0015\,(\text{exp})^{+0.0031}_{-0.0020}\,(\text{theo})$.

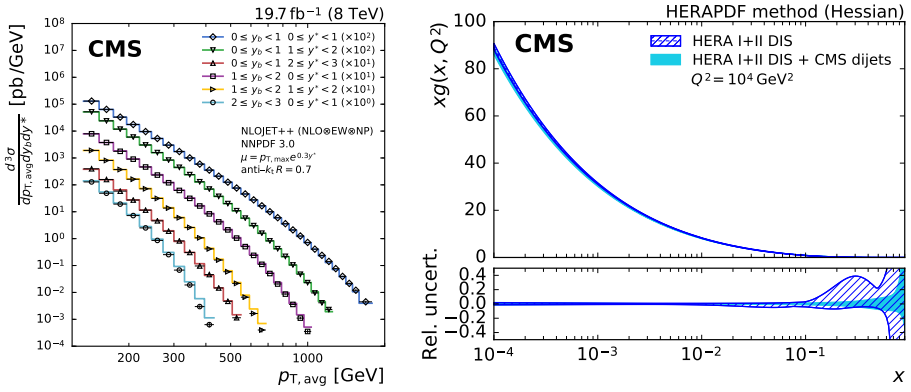

Figure 3: [8] Left : Triple-differential dijet cross sections in six bins of $y^\star$ and y_b are presented. The data are indicated by different markers for each bin. The theoretical predictions, obtained with NLOJET++ and NNPDF 3.0, and complemented with EW and NP corrections, are depicted by solid lines. Apart from the boosted region, the data are well described by the predictions at NLO accuracy over many orders of magnitude. Right : The gluon PDFs as a function of x at the scale $Q^2 = 10^4$ GeV^2, as derived from HERA inclusive DIS data alone (hatched band) [6] and in combination with CMS dijet data (solid band).

4. Inclusive multijets

The investigation of inclusive multijet event cross sections $\left(\sigma^i_{jet} \propto \alpha^i_S\right)$ as a function of jet p_T and rapidity y provides essential information about the PDFs and α_S. Moreover, the cross section ratios $R_{mn} = \frac{\sigma_{m-jet}}{\sigma_{n-jet}} \propto \alpha^{m-n}$, with $m > n$, provide an ideal tool to determine $\alpha_s(M_Z)$ as numerous theoretical and experimental uncertainties cancel in the ratio. The inclusive 2- and 3-jet event cross sections as well as cross section ratio (R_{32}) have been measured as a function of the average transverse momentum, $H_{T,2}/2 = \frac{1}{2}(p_{T,1} + p_{T,2})$ of the two leading jets, using CMS data collected at $\sqrt{s} = 8$ TeV corresponding to an integrated luminosity of 19.7 fb^{-1} [9]. The ratio of the 3-jet over 2-jet event cross section R_{32} is calculated as a function of $H_{T,2}/2$ from the unfolded data for each bin in $H_{T,2}/2$ and is with the one from NLO pQCD using CT10 NLO PDF set corrected with NP corrections in Fig. 4 (left). A fit of R_{32} using the MSTW2008 PDF set, gives $\alpha_s(M_Z) = 0.1150 \pm 0.0010\,(\text{exp}) \pm 0.0013\,(\text{PDF}) \pm 0.0015\,(\text{NP})\,^{+0.0050}_{-0.0000}\,(\text{scale})$. As shown in Fig. 4 (right), this value is in agreement with the world average value of $\alpha_s(M_Z) = 0.1181 \pm 0.0011$ [10] as well as previous CMS and ATLAS determinations [5, 11, 12, 13, 14, 15].

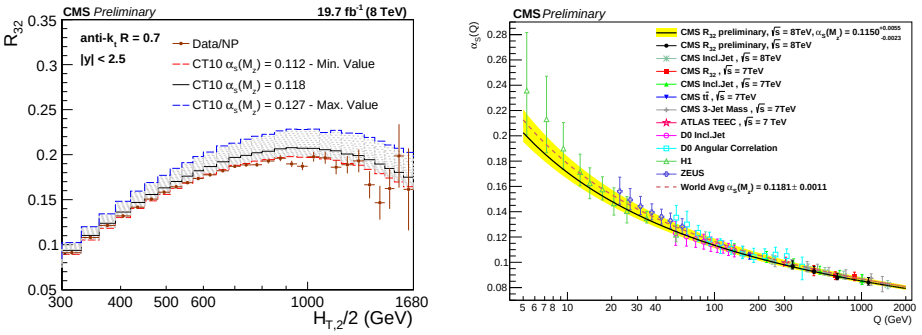

Figure 4: [9] Left : Cross section ratio R_{32} as a function of $H_{T,2}/2$ calculated from the data (solid circles) in comparison to that from NLO pQCD (lines). The NLO predictions using the CT10 NLO PDF set corrected with NP corrections are shown for a series of values assumed for $\alpha_s(M_Z)$ (dashed lines) together with the central prediction (solid line). Right : The running $\alpha_S(Q)$ as a function of the scale Q is shown. The evolution of the world average value of $\alpha_s(M_Z)$ [10] (dashed line) is shown along with other measurements of CMS [5, 11, 12, 13, 14], ATLAS [15], D0 [16, 17], H1 [18, 19], and ZEUS [20].

5. Azimuthal correlations

At leading order (LO) in pQCD, the two-final state partons are produced back-to-back in the transverse plane and thus the azimuthal angular separation between the two highest p_T jets in the transverse plane, $\Delta\phi_{1,2} = |\phi_{jet1} - \phi_{jet2}|$, equals π. The production of a third or more high-p_T jets leads to a deviation from π in the azimuthal angle. The measurement of the azimuthal angular correlation (or decorrelation from π) in multijet topologies is proven to be an interesting tool to test theoretical predictions of multijet production processes. The measurements of the normalized inclusive 2-jet, 3-jet, and 4-jet cross sections differential in $\Delta\phi_{1,2}$ and of the normalized inclusive 3-jet, and 4-jet cross sections differential in $\Delta\phi^{min}_{2j}$ (minimum azimuthal angular separation between any two of the three or four leading p_T jets,) have been performed for several regions in the leading-jet transverse momentum p_T^{max} [21]. The measurements are performed using the data collected

during 2016 corresponding to an integrated luminosity of 35.9 fb^{-1} of proton-proton collisions at $\sqrt{s} = 13$ TeV. The unfolded and normalized inclusive 2-jet (left), 3-jet (middle), and 4-jet (right) cross sections differential in $\Delta\phi_{1,2}$ are shown in Fig. 5 along with predictions from the PH-2J + PYTHIA8 event generator. In the 2-jet case the $\Delta\phi_{1,2}$ distributions are strongly peaked at π and become steeper with increasing p_T^{max}. In the 3-jet case, the $\Delta\phi_{1,2}$ distributions become flatter at π since the dijet events are missing and even more flat in the 4-jet case. The extension of $\Delta\phi_{1,2}$ correlations in inclusive 3-jet and 4-jet topologies are new results.

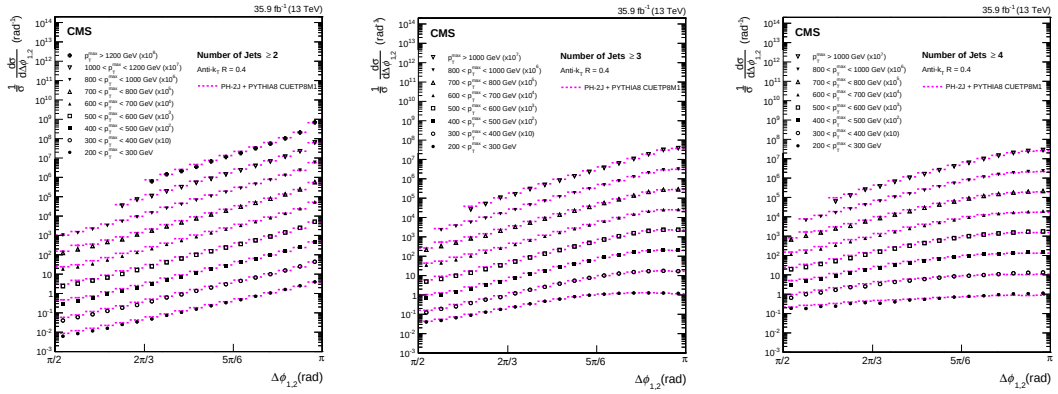

Figure 5: [21] Normalized inclusive 2-jet (left), 3-jet (middle) and 4-jet (right) cross section differential in $\Delta\phi_{1,2}$ for nine p_T^{max} regions, scaled by multiplicative factors for presentation purposes. Overlaid on the data are predictions from the PH-2J + PYTHIA8 event generator.

6. Summary

Jet production in proton-proton collisions is one of the main phenomenological predictions of perturbative Quantum Chromodynamics (pQCD). This paper summarizes the measurements of differential jet cross sections over a wide range in transverse momenta from inclusive jets to multi-jet final states [5, 7, 8, 9, 21]. The measurements are compared to theoretical predictions including those matched to parton shower and hadronization. These studies have an impact on the determination of the strong coupling α_S as well as on parton density functions [5, 8, 9].

References

[1] CMS Collaboration, JINST **3**, S08004 (2008).

[2] CMS Collaboration, JINST **12**, no. 10, P10003 (2017) arXiv:1706.04965 [physics.ins-det].

[3] M. Cacciari, G. P. Salam and G. Soyez, JHEP **0804**, 063 (2008) arXiv:0802.1189 [hep-ph].

[4] M. Cacciari, G. P. Salam and G. Soyez, Eur. Phys. J. C **72**, 1896 (2012) arXiv:1111.6097 [hep-ph].

[5] CMS Collaboration, JHEP **03**, 156 (2017) arXiv:1609.05331 [hep-ex].

[6] H1 and ZEUS Collaborations, Eur. Phys. J. C **75**, no. 12, 580 (2015) arXiv:1506.06042 [hep-ex].

[7] CMS Collaboration, Eur. Phys. J. C **76**, no. 8, 451 (2016) arXiv:1605.04436 [hep-ex].

[8] CMS Collaboration, Eur. Phys. J. C **77**, no. 11, 746 (2017) arXiv:1705.02628 [hep-ex].

[9] CMS Collaboration, CMS-PAS-SMP-16-008, http://cds.cern.ch/record/2253091

[10] Particle Data Group, Chin. Phys. C **40**, no. 10, 100001 (2016).

[11] CMS Collaboration, Eur. Phys. J. C **73**, no. 10, 2604 (2013) arXiv:1304.7498 [hep-ex].

[12] CMS Collaboration, Phys. Lett. B **728**, 496 (2014) arXiv:1307.1907 [hep-ex].

[13] CMS Collaboration, Eur. Phys. J. C **75**, no. 6, 288 (2015) arXiv:1410.6765 [hep-ex].

[14] CMS Collaboration, Eur. Phys. J. C **75**, no. 5, 186 (2015) arXiv:1412.1633 [hep-ex].

[15] ATLAS Collaboration, Phys. Lett. B **750**, 427 (2015) arXiv:1508.01579 [hep-ex].

[16] D0 Collaboration, Phys. Rev. D **80**, 111107 (2009) arXiv:0911.2710 [hep-ex].

[17] D0 Collaboration, Phys. Lett. B **718**, 56 (2012) arXiv:1207.4957 [hep-ex].

[18] H1 Collaboration, Eur. Phys. J. C **75**, no. 2, 65 (2015) arXiv:1406.4709 [hep-ex].

[19] H1 Collaboration, Eur. Phys. J. C **77**, no. 4, 215 (2017) arXiv:1611.03421 [hep-ex].

[20] ZEUS Collaboration, Nucl. Phys. B **864**, 1 (2012) arXiv:1205.6153 [hep-ex].

[21] CMS Collaboration, arXiv:1712.05471 [hep-ex].